Seizure Classification of EEG based on Wavelet Signal Denoising Using a Novel Channel Selection Algorithm

Niamh McCallan*‡, Scot Davidson*, Kok Yew Ng*†, Pardis Biglarbeigi*, Dewar Finlay*, Boon Leong Lan†, and James McLaughlin*
*NIBEC, Ulster University, Jordanstown Campus, Shore Road, Newtownabbey BT37 0QB, UK
†Electrical and Computer Systems Engineering, School of Engineering, Monash University, Malaysia
‡Corresponding author. Email: mccallan-n2@ulster.ac.uk

***Abstract*—Epilepsy is a disorder of the nervous system that can affect people of any age group. With roughly 50 million people worldwide diagnosed with the disorder, it is one of the most common neurological disorders. The electroencephalogram (EEG) is an indispensable tool for diagnosis of epileptic seizures in an ideal case, as brain waves from an epileptic patient would present distinct abnormalities. However, in real world situations there will often be biological and electrical noise interference, as well as the issue of a multi-channel signal, which introduce a great challenge for seizure detection and classification. For this study, the Temple University Hospital (TUH) EEG Seizure Corpus dataset was used. This paper proposes a novel channel selection method which isolates different frequency ranges within five channels. This is based upon the frequencies at which normal brain waveforms exhibit. A one second window was selected, with a 0.5 s overlap. Wavelet signal denoising was performed using Daubechies-4 wavelet decomposition. Thresholding was applied using minimax soft thresholding criteria. Filter banking was used to localise frequency ranges from five specific channels. Statistical features were then derived from the outputs. After performing bagged trees classification using 500 learners, a test accuracy of 0.82 was achieved.**

I. Introduction

Electroencephalogram (EEG) is widely used in different clinical settings, with the purpose of seizure detection and classification being the most abundant [16]. EEGs are used to measure electrical activities by means of placing many electrodes either on the exterior of the brain using a brain cap or via intracranial electrodes [22]. Epilepsy is characterised by recurrent, unpredictable and unprovoked seizures. People with epilepsy are known to have an increased risk of injury, unemployment, death, depression, anxiety, and other psychiatric and psychological issues [10]. Seizures are propagated when many neurons are synchronously excited, causing a wave of electrical activity in the brain [34]. There are many different orientations that can be used for the placement of the electrodes. However, the most common method is the International 10-20 System as shown in Figure 1. This is where 21 electrodes are evenly spaced across the scalp, with distances between each electrode equal to 10 % or 20 % of the total distance between nasion (front) and inion (back) [17]. This mapping is required because seizures can occur in a localised area (focal seizures) or more generally (generalised seizures). Focal seizures affect only one hemisphere of the brain and can be distinguished by whether or not awareness is retained. An example of a focal seizure is focal impaired aware seizure (FIAS), previously known as complex-partial seizure (CPSZ). This seizure type has a direct impact on a patient's ability to respond to any stimulus. The awareness of the patient is not retained during this period and the patient may appear disoriented or react abnormally [15]. Generalised seizures affect the majority, if not all, of the brain and can occur without provocation [27]. It is also typical for patients experiencing generalised seizures to lose consciousness or have uncontrolled muscle spasms. Tonic-clonic seizures (TCSZ) are the most well-known type of generalised seizure, in which the patient gets stiff and then jerks [15]. It is worth noting that many people experience only one type of seizure. However, some people may have various types of seizures. Additionally, the type of seizures that a patient has may alter over time [34].

The general practice for diagnosis of seizures involves a board certified EEG interpreter to examine patients and undertake manual EEG signal analysis for diagnosis, which is expensive and time consuming. This can also be exceedingly tiresome and place a significant physical and mental strain on physicians, as EEG recordings typically span several hours, with many patients being watched overnight or even for several days [28]. A detailed history from the patient and observers is required for an appropriate clinical diagnosis, which can be negatively affected by inaccurate and inadequate patient and witness histories. Recent research has revealed that even experienced neurologists have difficulty distinguishing between focal and generalised epilepsy [23]. According to the World Health Organisation (WHO), if provided with appropriate diagnosis and medication, up to 70 % of people with epilepsy could avoid seizure episodes [12]. As a result, substantial effort and research have gone into developing and implementing adequate seizure detection and classification algorithms to alleviate the clinical burden of manual EEG analysis [33]. The International League Against Epilepsy (ILAE) defines artefact as a physiological potential difference in an EEG recording caused by something other than the brain, such as eye movement, muscle movement, or muscular contractions; these are often referred to as biological artefacts. Additionally, recordings may be altered as a result of ambient electrical noise, and instrument distortion, or a malfunction; these are referred to as technical artefacts [20].

Early seizure detection methods rely on a variety of non-specific patient algorithms. More recently, research have focused on patient-specific algorithms to detect seizures with most findings obtaining accuracy ranging from 0.83–1.00 [2], [3]. Despite the excellent accuracy of these methods, the majority of seizure detection research studies have used the same dataset from the Department of Epileptology, University of Bonn. This dataset contains EEG recordings from 10 participants (Five without epilepsy and five with epilepsy) throughout a 23.5 s period [3]. Therefore, it is a limited dataset to be used for seizure detection. There have been much research carried out using the TUH Seizure Corpus dataset, with Lui et al. [23] achieving a F1-score of 0.97 and Roy et al. [27] reaching 0.91. An explanation for the terms accuracy and F1-score are available in Section II-G.

The purpose of this research is to focus on seizure detection and classification, using a large amount of annotated data. We provide a novel channel selection strategy that outperforms established methods. Additionally, our study demonstrates the feasibility of ensemble learning approaches over typical classification systems.

This paper is organised as follows: Section II introduces the dataset, how the signals are pre-processed alongside the novel channel selection algorithm used, feature extraction, selection and classification. It also describes the performance assessment used for this study. Section III presents the results and discussions gathered from this investigation. Section IV walks through a general conclusion of this study.

II. Method

This research considers three separate scenarios for seizure detection and classification; (1) detection of seizure and non-seizure periods, (2) focal-generalised-nonseizure classification, and (3) multi-classification using nonseizure periods (NNSZ), simple-partial seizures (SPSZ), CPSZ, tonic seizures (TNSZ), TCSZ, myoclonic seizures (MYSZ), and absence seizures (ABSZ).

A. Data Acquisition

Only a small amount of EEG datasets that focus on seizure detection and classification are available online, free and easily accessible such as the University of Bonn Dataset [6], CHB-MIT [32] and TUH-EEG [25]. With over 30,000 clinical EEG recordings collected over 18 years, starting in 2002 and currently ongoing, TUH Seizure Corpus has the largest publicly available dataset of EEG recordings. This dataset can be utilised for both academic and commercial purposes [29]. The reports comprise unstructured language that includes information on the patients' medical histories, medications, and clinical evaluations. Based on the neurologists' report and careful study of the signal, the annotation team was able to classify the types of seizures. The data include sessions from outpatient care, the intensive care unit (ICU), emergency multidisciplinary units (EMU), emergency room (ER), and a variety of other hospital settings. All data contain multi-channel signals ranging through 20–128 channels. A 16-bit A/D converter was used to digitise the data. The samples have a frequency range of 250–1024 Hz. More than 10 different electrode combinations and more than 40 channel configurations are included in the corpus [25].

TABLE I: TUH Seizure type file count.

Seizure Type	Total Count
Simple-Partial Seizures (SPSZ)	8
Complex-Partial Seizures (CPSZ)	162
Tonic Seizures (TNSZ)	28
Tonic-Clonic Seizures (TCSZ)	29
Myoclonic Seizures (MYSZ)	3
Absence Seizures (ABSZ)	20

For this study, TUH Seizure Corpus dataset v1.5.1 have been utilised. Only files containing six different seizure types namely: SPSZ, CPSZ, TNSZ, TCSZ, MYSZ, and ABSZ have been adopted for this investigation as shown in Table I. In 2017, the ILAE updated much of the terminology. For example, SPSZ is now referred to as Focal Aware Seizures (FAS) [15]. However, in this paper the terminology for the TUH Seizure Corpus dataset, as shown in Table I will be used. Our training set consists of 80 % of each seizure type and the remaining 20 % was used for testing.

B. Pre-processing

Since TUH Seizure Corpus has data collected from 250–1024 Hz, all signals were re-sampled to 256 Hz to ensure uniformity [23]. Only channels with EEG information were selected for further analysis. The first second of every signal was removed as it was found that this beginning segment often contains much noise. Low level frequency range, associated with respiratory artefact, and high level frequency information is often removed to limit the bandwidth, and noise of the signal. A first order band-pass Infinite Impulse Response (IIR) filter from 0.1–80 Hz was performed on the signals, followed by a 60 Hz notch filter used to remove power-line interference. This is most typically experienced as a result of a minor problem with disconnected electrodes, which involves immediate re-connection. Without the notch filter, the signal interference would likely lead to poor tracing quality [19]. Subsequently the signals were normalised so the range is in the interval of $[0, 1]$. This technique of signal normalisation is to scale EEG signals of all patients to the same amplitude levels [30]. Data were segmented into 1 s epochs with 0.5 s overlap. Findings of adjusting the window size clearly reveal that reducing the window size increases the likelihood of seizure detection [1]. Furthermore, studies demonstrate that by reducing the window size, predictive models can detect some peaks prior to the seizure onset. As a result, the smaller the window, the better the chance of predicting a seizure [1]. A Kaiser window was applied to the signals with a window

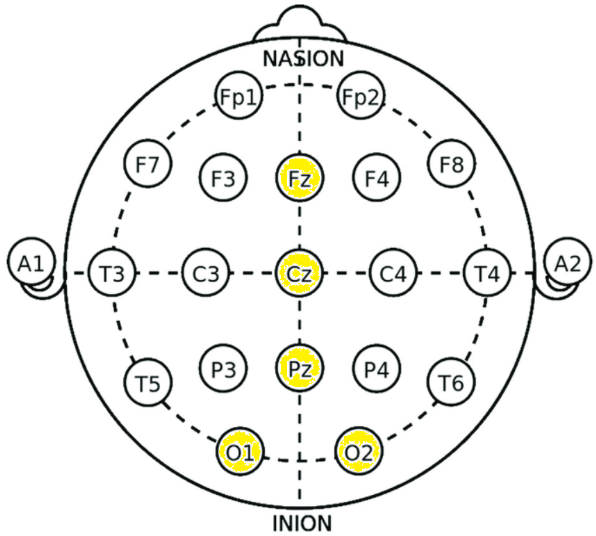

Fig. 1: EEG Electrode Configuration: International 10-20 System with selected channels described in Section II-C highlighted in yellow [26].

length of 1 s.

C. Channel Selection

A novel channel selection algorithm was created, which maps the areas of the brain where normal EEG waveforms in their specific frequency range should be found. The novelty of this channel selection method is that it is purely based on the regions of the brain that typical brain frequencies are dominant. This allows for further feature extraction to isolate the frequency ranges mentioned in Table II and discover if a pattern can be observed to differentiate nonseizure information against seizures. In Nayak et al. [24], it has been stated that the δ rhythm is prominent in the frontocentral head region. Due to light sleepiness, θ is most dominant in the frontocentral head regions and slowly migrates backward, replacing the α rhythm. For this reason, the frontal channel was selected as shown in Table II. In normal waking EEG recordings in the occipital head area, the posterior dominant α rhythm is typically present, hence the occipital channel was selected for feature extraction. The μ rhythm is a form of α rhythm that manifests itself in the central head regions and has an arch-like morphology. The frontocentral head areas are where σ waves are most noticeable. In normal adults and children, the β rhythm is the most common rhythm. It is most noticeable in the frontal and central head regions, and it gradually fades as it moves backward. Therefore, the posterior channel was selected as shown in Table II. Attempts to locate the γ rhythm have initiated a lot of research around the world, although no specific localisation has been discovered and it has been attributed to different areas in the brain [18]. In this study, the channels selected are: Central (CZ), Frontal (FZ), Posterior (PZ), Occipital (O1 and O2), as shown in Figure 1.

TABLE II: Channel Selection Criteria.

Frequency Band	Frequency Range (Hz)	Electrode Positioning
Delta, δ	0.1–4	FZ
Theta, θ	4–8	FZ
Alpha, α	8–13	O1, O2
Beta, β	14–30	FZ, PZ
Gamma, γ	30–80	CZ
Mu, μ	7–11	CZ
Slow Sigma, σ_s	12–14	FZ
Fast Sigma, σ_f	14–16	FZ

Principle Component Analysis (PCA) and Independent Component Analysis (ICA) have been used in this study to compare the viability of our novel channel selection method as they are some of the most popular methods used for dimenionality reduction [35]. PCA is an unsupervised method for mapping a dataset to specified feature vectors. It works by converting a high-dimensional dataset, such as multichannel EEG signals, into a low-dimensional orthogonal feature subspace, where each of the principal components is known. The variation of these principle components is organised in order of magnitude, with the first principle component having the most variance and the variance decreasing by an order of magnitude. This will limit the degrees of freedom as well as the complexities of space and time. The goal is to represent data in a space that accurately depicts variance in terms of sum-squared error. ICA is similar to PCA, but each signal is assumed to be a set of mutually independent signals. The multidimensional data is split into feature vectors that are statistically independent. [35].

D. Discrete Wavelet Denoising

Wavelet transform (WT) is a common approach for noise removal. Morley, a French researcher who focused their work on seismic data analysis, began research based on the idea of wavelet transforms in the early 1980s [14]. Farge et al. [14] contains a comprehensive description of many types of wavelet analysis methods, such as Continuous Wavelet Transforms (CWT)s and Discrete Wavelet Transforms (DWT)s. WT methods have been utilised by many researchers to reduce ocular artefacts (OA) [4], [37], [21]. Wavelet transforms can provide high frequency resolution at low frequencies whilst also providing high time resolution at high frequencies.

The DWT of a signal $x[n]$ is composed of approximation coefficients, $W\phi[j_0, k]$, and detail coefficients, $W\varphi[j_0, k]$ [9]. The approximation coefficients of signals represent the low-frequency components derived from the original signal's low-pass filter, whilst the detail coefficients are obtained by passing the signal through a high-pass filter at a higher level. To compute the detail and approximation coefficients at a lower level, the signal is down-sampled by two at each level. For a multi-level decomposition, this tree structure is repeated as shown in Figure 2. For the objectives of noise reduction of the EEG data, a 4-level wavelet decomposition using the 'db4' Daubechies wavelet as the mother wavelet was selected. With the noise estimate being level dependent, Minimax soft

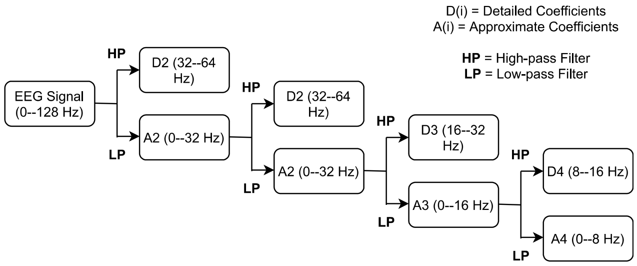

Fig. 2: A 4-level DWT.

thresholding was adopted. Minimax is a global thresholding method developed by Donoho and Johnstone [11]. This criteria is based on minimax principle that is used in statistics.

E. Filter Banking

From the five channels selected in Figure 1, 10 features where extracted by means of filter banking based on the criteria shown in Table II. A first order bandpass filter was used to split the various frequency bands.

F. Feature Selection and Classification

Following feature extraction, statistical analysis of each 1 s epoch of all 10 channels was undertaken to further reduce the dimensionality of the dataset. The statistics utilised include; maximum, minimum, root-mean-square (RMS), variance, standard deviation, log energy, normalised entropy, and maximum frequency. Patient age is also used as a feature, due to its general importance in seizure diagnosis [34]. The equations of these statistics are as follows:

1) RMS: The RMS level of a vector x is defined as:

$$x_{RMS} = \sqrt{\frac{1}{N}\sum_{n=1}^{N}|x_n|^2} \tag{1}$$

with the summation taking place along the chosen dimension.

2) Variance: For a random variable vector A made up of N scalar observations, the variance is:

$$V = \frac{1}{N-1}\sum_{i=1}^{N}|A_i - \mu_A|^2 \tag{2}$$

where μ is the mean of A and it is written using:

$$\mu_A = \frac{1}{N}\sum_{i=1}^{N}A_i \tag{3}$$

Some definitions of variance use a normalisation factor of N instead of $N-1$. In either scenario, the typical normalisation factor N is assumed for the mean.

3) Standard Deviation: The standard deviation is the square root of the variance and it is written using:

$$S = \sqrt{\frac{1}{N-1}\sum_{i=1}^{N}|A_i - \mu_A|^2} \tag{4}$$

4) Log Energy: Log energy is defined as:

$$\begin{aligned} LE(s_i) &= \log(s_i^2) \\ LE(s) &= \sum i \log(s_i^2) \end{aligned} \tag{5}$$

where the convention $\log(0) = 0$ is assumed. The signal is s and s_i^2 the coefficients of s in an orthonormal basis.

5) Normalised Entropy: The concentration in l^p norm entropy, where $p = 1.1$. The equation for normalised entropy is:

$$\begin{aligned} NE(s_i) &= |s_i|^p \\ NE(s) &= \sum i|s_i|^p = ||s||_p^p \end{aligned} \tag{6}$$

where s is the signal and s_i^2 the coefficients of s in an orthonormal basis.

6) Maximum Frequency: The maximum frequency is achieved firstly by getting the Fast Fourier Tranform (FFT) of each epoch and it can be expressed using:

$$Y(k) = \sum_{j=1}^{n} X(j)W_n(j-1)(k-1) \tag{7}$$

where

$$W_n = e^{(-2\pi i)/n} \tag{8}$$

The absolute values are then obtained using the following equation:

$$abs = \sqrt{Imag^2 + Real^2} \tag{9}$$

Before classification of this data could begin, some post-processing was required as the dataset was completely unbalanced, with the large majority of labels being nonseizure periods. Therefore, an algorithm was implemented to balance out this dataset, where the total count of seizure and nonseizure periods were tallied. Any addition labels beyond the mean where removed at random.

Ensemble bagged trees (EBT), otherwise known as Bootstrap is a prominent ensemble machine learning method that has previously demonstrated its efficiency in a variety of real-world categorisation problems. EBT was first developed by Breiman in 1996 [7]. It teaches a set of classifiers how to classify a new object [8]. Bagging is a technique for combining classifiers to achieve higher accuracy than a single classifier. Using bootstrap re-sampling, the EBT classifier separates the training data into subsets. Each subset is used as training data to build each decision tree. The bootstrapping number determines the number of decision trees that are built. The outputs of the decision trees are then used in the majority of voting stage. This model generates an ensemble of simple decision trees [13].

For this study, EBT classification was used with 500 learning cycles, after which k-fold cross validation was then performed using 10 sub-samples. The k-fold cross-validation algorithm divides all samples into k sub-samples at random. A sub-sample is validated using k sub-samples, and the linked classifier is tested using the remaining $k-1$ sub-samples. This method is carried out k times in total. For verification, each sub-sample is utilised only once. The average of k outcomes is then used to calculate a single result. As a result, all samples collected by randomly repeated sub-sampling can be used for both training and validation [13].

The k-nearest neighbour classifier has been used in this study as a comparison classifier against EBT classification. It is a simple, nonparametric, and nonlinear classifier [31]. It is based on the similarity measure between the training and test dataset. The training sets create the n-dimensional pattern space, and each set represents a point in n-dimensional space. Based on nearby k training data, test/unknown data are allocated to the class. Eq. (10) is used to calculate the 'nearness' of the dataset.

$$ED = \sqrt{\sum_{i=1}^{n} (Y_{1i} - Y_{2i})^2} \tag{10}$$

where

$$Y_{1i} = (y_{1_1}, y_{1_2}, \ldots, y_{1_n}) \text{ and } Y_{2i} = (y_{2_1}, y_{2_2}, \ldots, y_{2_n}) \tag{11}$$

Before doing the computation on ED, the values of each attribute can be normalised. The classifier generally uses a majority vote from the k-nearest neighbours instead of using the single closest dataset. The value of k, the number of neighbours with the lowest error rate, has been set to eight [31]. Considering that k-NN is a distance based algorithm, the distance calculation has an impact on classification performance. The distance metric, which is a mathematical representation that determines the distance between two data points, is used to calculate the distance. For this study, cityblock was selected as the distance metric, in which the distance between two points in a fixed Cartesian coordinate system is measured [36] as shown in Eq. (12) below

$$D_{city} = |x_1 - x_2| + |y_1 - y_2| \tag{12}$$

where the distance weight was set such that $w_D = 1/D_{city}^2$.

G. Performance Assessment

Sensitivity, specificity, accuracy, and F1-score are the most often used performance measures in signal processing to evaluate the performance of an algorithm. The following equations are used to describe these metrics:

$$Sensitivity = \frac{TP}{TP + FN} \tag{13}$$

$$Specificity = \frac{TN}{TN + FP} \tag{14}$$

$$Accuracy = \frac{TP + TN}{TN + FP + TP + FN} \tag{15}$$

$$Precision = \frac{TP}{TP + FP} \tag{16}$$

$$F1 - Score = \frac{2 * Precision * Sensitivity}{Precision + Sensitivity} \tag{17}$$

where TP is the number of seizure periods that have been detected by both a human expert and the algorithm, and FN is the number of seizure periods that have been determined by a human expert but have not been discovered by the algorithm. The number of nonseizure periods detected by both a human expert and the algorithm is represented by TN, and FP defines the number of nonseizure periods that the algorithm detected as seizure but were not recognised as such by a human expert [5].

TABLE III: Three tables depicting test results for seizure detection and classification.

Method	Sensitivity	Specificity	Accuracy	F1-Score
Novel Channel Selection				
EBT	**0.75**	**0.75**	**0.82**	**0.73**
k-NN	0.73	0.73	0.77	0.68
ICA				
EBT	0.57	0.57	0.78	0.58
k-NN	0.56	0.56	0.66	0.54
PCA				
EBT	0.62	0.62	0.74	0.61
k-NN	0.55	0.55	0.55	0.49

(a) Performance metrics for Scenario 1: Detection using the novel channel selection method, ICA, and PCA.

Method	Sensitivity	Specificity	Accuracy	F1-Score
Novel Channel Selection				
EBT	0.59	0.77	**0.68**	**0.61**
k-NN	**0.64**	**0.79**	0.51	0.47
ICA				
EBT	0.47	0.74	0.40	0.32
k-NN	0.37	0.69	0.31	0.25
PCA				
EBT	0.50	0.73	0.35	0.30
k-NN	0.42	0.69	0.31	0.25

(b) Performance metrics for Scenario 2: Focal-generalised-nonseizure Classification using the novel channel selection method, ICA, and PCA.

Method	Sensitivity	Specificity	Accuracy	F1-Score
Novel Channel Selection				
EBT	**0.55**	**0.93**	**0.69**	**0.51**
k-NN	0.46	0.91	0.53	0.41
ICA				
EBT	0.26	0.89	0.47	0.47
k-NN	0.21	0.87	0.33	0.12
PCA				
EBT	0.27	0.88	0.45	0.45
k-NN	0.25	0.87	0.32	0.32

(c) Performance metrics for Scenario 3: Multi-classification using the novel channel selection method, ICA, and PCA.

III. Experimental Results and Discussion

Comparing the EBT method against k-NN classification, the EBT method clearly outperforms k-NN in all the scenarios explored in this study. From the results presented in Table III, it is clear too that our novel channel selection method outperforms both ICA and PCA.

Figure 4a demonstrates a confusion chart of the results gathered from Scenario 1: seizure detection, where the classifier is able to accurately detect 0.86 of nonseizure periods and 0.65 of seizure periods, with an overall accuracy of 0.82, the highest results from this investigation. The poorest accuracy and F1-score are from using PCA with k-NN at 0.55 and 0.49, respectively, as shown in Table IIIa. The true positive rate of seizure detection is quite low but with few false positives.

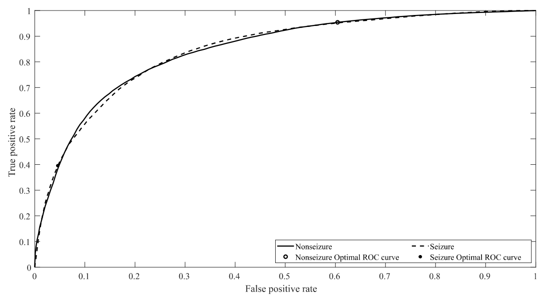

(a) Seizure Detection (Scenario 1).

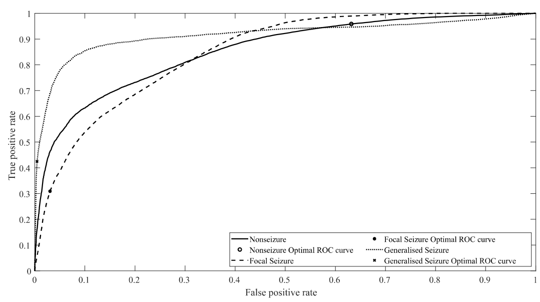

(b) Focal, general and nonseizure classification (Scenario 2).

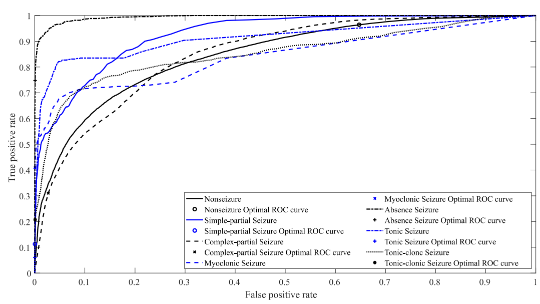

(c) Multi-classification (Scenario 3).

Fig. 3: Three ROC curve graphs of test performance results for seizure detection and classification from novel channel selection algorithm using EBT classifier.

Nonseizure detection has a higher true positive rate but also a high false positive rate as indicated by the optimal ROC curve point in Figure 3a.

Considering Scenario 2: focal-generalised-nonseizure classification as shown in Figure 4b, and Table IIIb, the superiority of using the combination of the novel channel selection method and EBT classification is evident with an accuracy and F1-score of 0.68 and 0.61, respectively. It is important to note that there are more cases of nonseizure periods being incorrectly classified as focal seizures as shown in Figure 4b. In this setting however, it seems that using the combination of ICA and k-NN produced the poorest results with an accuracy and F1-score of 0.31 and 0.25, respectively. Although these results are the same when using the combination of PCA

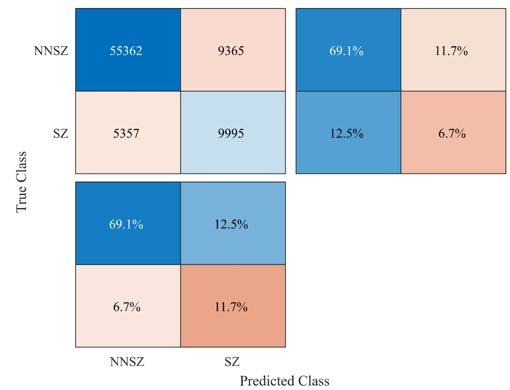

(a) Confusion matrix depicting seizure (SZ) vs nonseizure (NNSZ) results (Scenario 1).

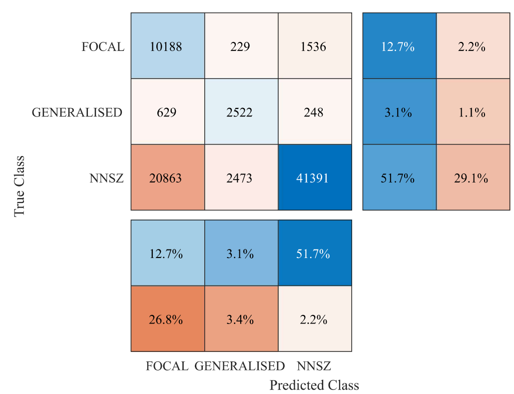

(b) Confusion matrix depicting focal seizure, generalised seizure vs nonseizure results (Scenario 2).

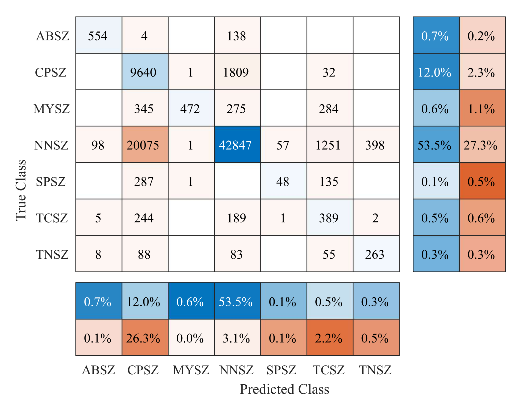

(c) Confusion matrix depicting multi-classification (Scenario 3).

Fig. 4: Three confusion matrices of test performance results for seizure detection and classification from novel channel selection algorithm using EBT classifier.

and k-NN, in this circumstance, the sensitivity results are the lowest at 0.37. From Figure 3b, it it shown that the ROC curve for generalised seizure classification has the highest true positive rate. Generalised seizures have an extremely low false positive rate, however the optimal ROC point indicates that the true positive rate is quite low at just above 0.40. This classifier performs well for nonseizure classification, however there is a trade-off in the ROC curve due to the high false positive rate. Therefore, it is likely nonseizure periods are being overly misclassified and the model could be overfit. Focal seizures have the lowest levels of true positive detection rates and the true positive rate is also extremely low. Focal seizures fall closest to the diagonal line of the ROC graph, indicating that these results are likely random.

In the setting of multi-classification, overall accuracy has actually improved when comparing with focal-generalised-nonseizure classification. The novel channel selection algorithm using EBT classifier still achieved the best results with an accuracy and F1-score of 0.69 and 0.51, respectively. In this case, the poorest results are again gathered using ICA with k-NN with an accuracy and F1-score of 0.33 and 0.12, respectively. Interestingly from Figure 4c, it can be observed to a greater extend than in Figure 4b that a relatively high quantity of nonseizure periods are being incorrectly identified. The confusion chart allows us to establish that the classifier incorrectly identifies some of these nonseizure cases as complex-partial seizures.

The trend for nonseizure classification in Scenario 3: multi-classification, closely resembles that of the other classification scenarios with both a high true positive rate and high false positive rate, possibly meaning that there is an overfitting issue with nonseizure classification as shown in Figure 3c. It can be noted that simple-partial, tonic, and tonic-clonic seizures have a very low true positive and false positive rate, possibly outlining the need for more data, as these classes are underrepresented. It is observed that the ROC curve for absence seizures falls closely to the perfect classifier margin, with a high true positive rate and virtually no false positive detection, also evident from Figure 4c. This pattern closely matches that of the ROC curve for generalised seizure classification in Figure 3b, indicating the greatest barrier of this work is creating a functional model to classify focal seizures, specifically complex-partial seizures. Myoclonic classification did not perform effectively, with slightly more true positive detection than false positive. Simple-partial seizure classification was not adequate, with again more false positives. Only complex-partial and absence seizure classification performed to an acceptable range.

IV. Conclusions

The main challenge that exists today is obtaining an accurate automated seizure classification model that can differentiate between various seizure types to overcome the clinical burden of manual EEG analysis. This paper has presented the application of using our novel channel selection method based on frequency information dependent to specific regions of a normal brain. From the results presented, it can be noted that this method does successfully isolate the information found in an abnormal brain during seizure occurrences. It is evident that using this channel selection method combined with the EBT classification model outperforms other commonly used methods for seizure detection, with the highest accuracy of 0.82. From this experiment, it has also been discovered that there are difficulties with classification models when differentiating nonseizure periods from complex-partial seizures. The results from the confusion matrices in Figure 4 provide the following summary:

- Figure 4a — many nonseizures being misclassified as seizures,
- Figure 4b — many nonseizures being misclassified as focal seizures,
- Figure 4c — many nonseizures being misclassified as complex-partial seizures.

Potential future work will involve researching possible methods to isolate nonseizure periods from complex-partial seizures. Furthermore, this work has proved promising in terms of multi-classification of the various seizure types. Future work can focus on improving this current methodology, with the possibility of moving more into deep learning methods to classify the various seizure types. Our novel channel selection method with long short-term memory or various deep learning methods may provide better results, as there has been promising results recently using long short-term memory in seizure classification [16]. It can also be noted that results gathered from Scenario 3 are not much different from Scenario 2, therefore we will redact Scenario 2 from any future work.

References

[1] Abbaszadeh B, Yagoub MC. Optimum Window Size and Overlap for Robust Probabilistic Prediction of Seizures with iEEG. In 2019 *IEEE Conference on Computational Intelligence in Bioinformatics and Computational Biology (CIBCB)* 2019 Jul 9 (pp. 1–5). IEEE.

[2] Acharya UR, Hagiwara Y, Adeli H. Automated Seizure Prediction. *Epilepsy & Behavior*. 2018 Nov 1;88:251–261.

[3] Acharya UR, Sree SV, Swapna G, Martis RJ, Suri JS. Automated EEG Analysis of Epilepsy: A Review. *Knowledge-Based Systems*. 2013 Jun 1;45:147–165.

[4] Al-Qazzaz NK, Ali S, Ahmad SA, Islam MS, Ariff MI. Selection of Mother Wavelets Thresholding Methods in Denoising Multi-channel EEG Signals During Working Memory Task. In 2014 *IEEE Conference on Biomedical Engineering and Sciences (IECBES)* 2014 Dec 8 (pp. 214–219). IEEE.

[5] Alotaiby TN, Alshebeili SA, Alshawi T, Ahmad I, Abd El-Samie FE. EEG Seizure Detection and Prediction Algorithms: A Survey. *EURASIP Journal on Advances in Signal Processing.* 2014 Dec;2014(1):1–21.

[6] Andrzejak RG, Lehnertz K, Mormann F, Rieke C, David P, Elger CE. Indications of Nonlinear Deterministic and Finite-dimensional Structures in Time Series of Brain Electrical Activity: Dependence on Recording Region and Brain State. *Physical Review E.* 2001 Nov 20;64(6):061907.

[7] Breiman L. Bagging predictors. *Machine learning.* 1996 Aug;24(2):123–140.

[8] Das T, Ghosh A, Guha S, Basak P. Classification of EEG Signals for Prediction of Seizure using Multi-feature Extraction. In 2017 *1st International Conference on Electronics, Materials Engineering and Nano-Technology (IEMENTech)* 2017 Apr 28 (pp. 1–4). IEEE.

[9] Daubechies I. The Wavelet Transform, Time-frequency Localization and Signal Analysis. *Princeton University Press*; 2009 Jan 10.

[10] De Boer HM, Mula M, Sander JW. The Global Burden and Stigma of Epilepsy. *Epilepsy & Behavior.* 2008 May 1;12(4):540–546.

[11] Donoho DL, Johnstone IM. Minimax Estimation via Wavelet Shrinkage. *The Annals of Statistics.* 1998;26(3):879–921.

[12] Epilepsy [Internet]. *Who.int.* 2021 [cited 7 June 2021]. Available from: https://www.who.int/news-room/fact-sheets/detail/epilepsy

[13] Erdamar A, Aksahin MF. Quantitative Sleep EEG Synchronization Analysis for Automatic Arousals Detection. *Biomedical Signal Processing and Control.* 2020 May 1;59:101895.

[14] Farge M. Wavelet Transforms and their Applications to Turbulence. *Annual Review of Fluid Mechanics.* 1992 Jan;24(1):395–458.

[15] Fisher RS, Cross JH, French JA, Higurashi N, Hirsch E, Jansen FE, Lagae L, Moshé SL, Peltola J, Roulet Perez E, Scheffer IE. Operational Classification of Seizure Types by the International League Against Epilepsy: Position Paper of the ILAE Commission for Classification and Terminology. *Epilepsia*. 2017 Apr;58(4):522–530.

[16] Golmohammadi M, Ziyabari S, Shah V, de Diego SL, Obeid I, Picone J. Deep Architectures for Automated Seizure Detection in Scalp EEGs. *arXiv preprint arXiv:1712.09776*. 2017 Dec 28.

[17] Homan RW, Herman J, Purdy P. Cerebral Location of International 10–20 System Electrode Placement. *Electroencephalography and Clinical Neurophysiology.* 1987 Apr 1;66(4):376–382.

[18] Jia X, Kohn A. Gamma Rhythms in the Brain. *PLoS Biology*. 2011 Apr 12;9(4):e1001045.

[19] Jiang X, Bian GB, Tian Z. Removal of Artefacts from EEG Signals: A Review. *Sensors.* 2019 Jan;19(5):987.

[20] Kane N, Acharya J, Beniczky S, Caboclo L, Finnigan S, Kaplan PW, Shibasaki H, Pressler R, van Putten MJ. A Revised Glossary of Terms Most Commonly used by Clinical Electroencephalographers and Updated Proposal for the Report Format of the EEG Findings. Revision 2017. *Clinical Neurophysiology Practice*. 2017;2:170.

[21] Krishnaveni V, Jayaraman S, Aravind S, Hariharasudhan V, Ramadoss K. Automatic Identification and Removal of Ocular artefacts from EEG using Wavelet Transform. *Measurement Science Review.* 2006 Nov;6(4):45–57.

[22] Light GA, Williams LE, Minow F, Sprock J, Rissling A, Sharp R, Swerdlow NR, Braff DL. Electroencephalography (EEG) and Event-related Potentials (ERPs) with Human Participants. *Current Protocols in Neuroscience.* 2010 Jul;52(1):6–25.

[23] Liu T, Truong ND, Nikpour A, Zhou L, Kavehei O. Epileptic Seizure Classification with Symmetric and Hybrid Bilinear Models.*IEEE Journal of Biomedical and Health Informatics.* 2020 Apr 2;24(10):2844–2851.

[24] Nayak CS, Anilkumar AC. EEG Normal Waveforms. *StatPearls [Internet].* 2020 Jun 28.

[25] Obeid I, Picone J. The Temple University Hospital EEG Data Corpus. *Frontiers in Neuroscience.* 2016 May 13;10:196.

[26] Rojas, G. M., Alvarez, C., Montoya, C. E., de la Iglesia-Vayá, M., Cisternas, J. E., and Gálvez, M. (2018). Study of Resting-state Functional Connectivity Networks Using EEG Electrodes Position as Seed. *Frontiers in Neuroscience*, 12, 235.

[27] Roy S, Asif U, Tang J, Harrer S. Machine Learning for Seizure Type Classification: Setting the Benchmark. *arXiv preprint arXiv:1902.01012.* 2019.

[28] Saab K, Dunnmon J, Ré C, Rubin D, Lee-Messer C. Weak Supervision as An Efficient Approach for Automated Seizure Detection in Electroencephalography. *NPJ Digital Medicine.* 2020 Apr 20;3(1):1–12.

[29] Shah V, Von Weltin E, Lopez S, McHugh JR, Veloso L, Golmohammadi M, Obeid I, Picone J. The Temple University Hospital Seizure Detection Corpus. *Frontiers in Neuroinformatics.* 2018 Nov 14;12:83.

[30] Sharma R, Chopra K. EEG-based Epileptic Seizure Detection using GPLV Model and Multi Support Vector Machine. *Journal of Information and Optimization Sciences.* 2020 Jan 2;41(1):143–161.

[31] Sharmila A, Geethanjali P. DWT Based Detection of Epileptic Seizure from EEG Signals using Naive Bayes and k-NN Classifiers. *IEEE Access.* 2016 Jun 30;4:7716–7727.

[32] Shoeb AH. Application of Machine Learning to Epileptic Seizure Onset Detection and Treatment *(Doctoral dissertation, Massachusetts Institute of Technology).*

[33] Sriraam N, Raghu S, Tamanna K, Narayan L, Khanum M, Hegde AS, Kumar AB. Automated Epileptic Seizures Detection using Multi-features and Multilayer Perceptron Neural Network. *Brain Informatics.* 2018 Dec;5(2):1–10.

[34] Stafstrom CE, Carmant L. Seizures and Epilepsy: An Overview for Neuroscientists. *Cold Spring Harbor Perspectives in Medicine.* 2015 Jun 1;5(6):a022426.

[35] Subasi A, Gursoy MI. EEG Signal Classification using PCA, ICA, LDA and Support Vector Machines. *Expert Systems with Applications.* 2010 Dec 1;37(12):8659-8666.

[36] Yean CW, Khairunizam W, Omar MI, Murugappan M, Zheng BS, Bakar SA, Razlan ZM, Ibrahim Z. Analysis of the Distance Metrics of KNN Classifier for EEG Signal in Stroke Patients. In *2018 International Conference on Computational Approach in Smart Systems Design and Applications (ICASSDA)* 2018 Aug 15 (pp. 1–. IEEE.

[37] Zikov T, Bibian S, Dumont GA, Huzmezan M, Ries CR. A Wavelet Based De-noising Technique for Ocular artefact Correction of the Electroencephalogram. In Proceedings of the *Second Joint 24th Annual Conference and the Annual Fall Meeting of the Biomedical Engineering Society][Engineering in Medicine and Biology* 2002 Oct 23 (Vol. 1, pp. 98–105). IEEE.